arXiv:1109.0879v1 [physics.comp-ph] 30 Aug 2011

A new method to find full complex roots of a complex dispersion equation for light propagation

Li Wan*
Department of Physics, Wenzhou University, Wenzhou 325035, People's Republic of China

A new numerical method is presented to find full complex roots of a complex dispersion equation. For the application of the solution, the complex dispersion equation of a cylindrical metallic nanowire is investigated. By using this method, locus of Brewster angle, complex dispersion curves of Surface Plasmon Polaritons (SPPs) and complex bulk modes can be obtained in once calculation. Approximate analytical solution to the complex dispersion equation has also been derived to verify our method.

PACS numbers: 73.20.Mf, 41.20.-q, 41.20.Jb, 78.20.Bh

I. INTRODUCTION

Dispersion relation is the basic property of light propagating in mediums, which specifies the relation between the wavevector k and the frequency ω of the light. Recently, the light propagation in metallic nanostructures has attracted enormous attentions from researchers due to the excitation of the Surface Plasmon-polaritons(SPPs) [1–5] by the light. The SPPs are known for the wide application in nano optics attributed to the spatial localization of the SPPs at the metal-dielectric interfaces, which can be guided to manipulate light in nanoscaled photonic circuitry[1–5]. Furthermore, the spatial confinement of the SPPs can enhance the field intensity at the interfaces, which can influence the luminescence intensities[6–8] and life time of emitters close to the interfaces.[9,10] In order to understand the physical properties of SPPs in plasmonic structures, it is important to get the dispersion relations of light propagation in the plasmonic structures. Principally, the dispersion relations can be obtained by solving the Maxwell equations with the boundary conditions of the plasmonic structures imposed. For simple plasmonic structures, such as planar metal surfaces, the dispersion of SPPs can be solved analytically.[11–14] But for the most structures which are nonsymmetrical and irregular, codes such as finite-element method (FEM) and finite-difference time-domain techniques (FDTD) need to be applied for numerical calculations. The basic technique of FEM or FDTD is to discrete the Maxwell equations, which are known for the time consumption. Fortunately, for some symmetric structures, such as cylindrical nanowires,[11,15–19] the Maxwell equations imposed with the boundary conditions can be transformed into a dispersion equation. Solving the dispersion equation can improve the efficiency to get the dispersion relation rather than the numerical calculation by the discretion of Maxwell equations.

The dispersion equation normally is nonlinear and transcendental. What is more, when the metal loss is introduced into the metal dielectric,[13,14,20,21] the dispersion equation then is a complex and transcendental equation. Thus, the dispersion relations obtained from the complex equation are also complex. There exist two types of the complex dispersion relations for one same plasmonic structure, specifying either a complex frequency as a function of a real wave vector, noted as $complex-\omega$ for convenience, or a complex wave vector as a function of a real frequency, noted as $complex-k$. The two types of dispersion relations are rather different, even though they are for one same structure. The back bending as a characteristic of the $complex-k$ relation is absent in the $complex-\omega$ relation. The latter is an asymptotic curve.[18,19] It has been suggested that the $complex-k$ solution of the dispersion relation describes the SPPs mode decaying spatially while the $complex-\omega$ solution is for the SPPs decaying in time rather than in space.[12,22,23] The discrepancy of the two solutions has been considered to be originated from the metal Ohmic loss.[13,14,20,21] Such conclusion is originally drawn from the study of SPPs on planar metallic-dielectric surfaces. When a perfect metal without damping is considered in this planar case, the two types of solutions of the SPPs dispersion relations overlap with a same asymptotic behavior. When the metal Ohmic loss is introduced into the dielectric response of metal, the two types of solutions are then different. The original of the discrepancy of the two solutions due to the metal loss has also been confirmed in cylindrical metallic nanowires.[24]

The main mission to get the dispersion relation of the light propagation in plasmonic structures then is to find the complex roots of the equation. The complex dispersion equation can be described by $f(x,y,z)=0$ with three real variables x, y and z. For example, in the $complex-\omega$ solution, x, y and z represent the real part of ω ($Re[\omega]$), the imaginary part of ω ($Im[\omega]$) and real wavevector k respectively. In the $complex-k$ solution, x, y and z then represent the real part of k ($Re[k]$), imaginary part of k ($Im[k]$) and real ω respectively. To solve this complex equation, normally one variable is given, say z, then the complex equation can be simplified to be a complex equation $f(x,y)=0$ with only two real variables. One commonly used method to solve this equation is to choose all possible values of x and y in their given ranges to check if they satisfy the equation or not. To achieve this purpose, a coordination system with x and y axis is gridded with an enough small mesh size and then the values of x and y at each grid point are substituted into the equation. Considering the error allowance δ, the criterion for this grid method is to find the roots (x_0,y_0) if they satisfy $|f(x_0,y_0)|<\delta$. To this grid method, there exit two main short comings. The first is that in order to get the full solutions to the equation, one needs to gird the coordinate system with an enough small mesh size. Or, the solutions may be lost. However, in the reality for the calculation, we find that the mesh size can reach the order of the magnitude of 10^{-15} and even smaller, which increases the computation time. The second shortcoming is that the criterion can not

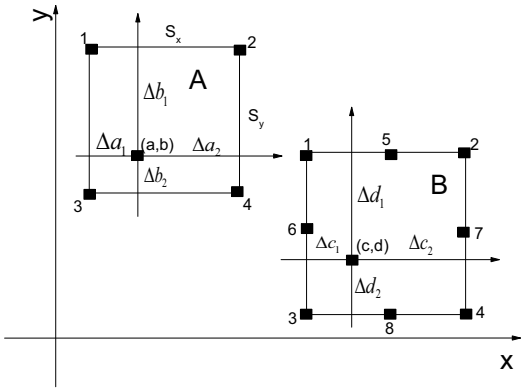

FIG. 1: Schematic of our method to get full complex roots of a complex dispersion equation. S_x and S_y are the mesh sizes along x and y axis respectively. (a, b) and (c, d) are assumed to be the roots of the equation, enclosed in mesh A and mesh B respectively. The former is used for the linear approximation, while the latter is for the parabola approximation.

guarantee the (x_0, y_0) to be the root even though they satisfy the criterion since δ is not rigorously equal to zero. No matter how small the δ is taken, the second shortcoming still remains since $\delta \neq 0$. To improve the computation efficiency, the alternative method is the Newton-Raphson (NR) method, which can converge to the roots of the equation quickly. However, it is well known that the NR method may miss the roots if there exist multiroots of the equation. What is more, the NR method may not converge if the initial estimate is not close enough to the root, or may converge to wrong root. Especially for the complex transcendental equation, which is very common for the light propagation in plasmonic structures when the metal Ohmic loss is introduced, the NR method will lose its power to find the roots. In this paper, we propose one new method to find full complex roots of complex transcendental equations. As an example for the application, the dispersion equation of light propagating in a cylindrical metallic nanowire is investigated.

II. METHOD

A. linear approximation

The main mission of our method to solve the complex equation $f(x, y) = 0$ is to find criterions used to judge if the values of the variables are the roots or not. Similarly to the grid method, the coordination system with x and y axis is gridded firstly. Suppose that a and b are the roots of the equation satisfying $f(a, b) = 0$ and the point (a, b) is enclosed in the mesh A(fig. 1), then the function at each point of the mesh corner can be expanded at the point (a, b) by the first order Taylor series as

$$f(x,y)_1 = f(a,b) + f'_x(a,b)(-\triangle a_1) + f'_y(a,b)(\triangle b_1), \quad (1a)$$

$$f(x,y)_2 = f(a,b) + f'_x(a,b)(\triangle a_2) + f'_y(a,b)(\triangle b_1), \quad (1b)$$

$$f(x,y)_3 = f(a,b) + f'_x(a,b)(-\triangle a_1) + f'_y(a,b)(-\triangle b_2), \quad (1c)$$

$$f(x,y)_4 = f(a,b) + f'_x(a,b)(\triangle a_2) + f'_y(a,b)(-\triangle b_2). \quad (1d)$$

Here, subscript j of $f(x,y)_{j(j=1,2,3,4)}$ represents the calculated results of the function $f(x,y)$ at the corner point $j(j = 1, 2, 3, 4)$ of mesh A, which has been labeled in the fig. 1. The complex $f'_{x(y)}(a,b)$ is the partial derivative of the function with respect to $x(y)$ at the point of (a,b). $\triangle a_1$, $\triangle a_2$, $\triangle b_1$, and $\triangle b_2$ are the absolute values of the coordination components of the four corner points of the mesh A with respect to the point (a,b) considered as the coordinate origin. Eq.(1a) subtracted from eq.(1b) gives

$$f'_x(a,b) = \frac{f(x,y)_2 - f(x,y)_1}{\triangle a_1 + \triangle a_2} = \frac{f(x,y)_2 - f(x,y)_1}{S_x}, \quad (2a)$$

and eq.(1a) subtracted from eq.(1c) gives

$$f'_y(a,b) = \frac{f(x,y)_1 - f(x,y)_3}{\triangle b_1 + \triangle b_2} = \frac{f(x,y)_1 - f(x,y)_3}{S_y}. \quad (2b)$$

The S_x and S_y are the mesh sizes along the x and y axis respectively, which are given as constants when gridding the coordination system. We substitute eq.(2) into eq.(1a), obtaining

$$\triangle a_1 = \frac{L_2 L_{12} - L_1 L_{22}}{L_{21} L_{12} - L_{11} L_{22}}, \quad (3a)$$

$$\triangle b_1 = \frac{L_1 L_{21} - L_2 L_{11}}{L_{21} L_{12} - L_{11} L_{22}}, \quad (3b)$$

with

$$L_1 = Re[f(x,y)_1], \quad L_2 = Im[f(x,y)_1], \quad L_{11} = Re[-f'_x(a,b)],$$
$$L_{12} = Re[f'_y(a,b)], \quad L_{21} = Im[-f'_x(a,b)], \quad L_{22} = Im[f'_y(a,b)].$$

Similarly, by substituting eq.(2) into eq.(1b), (1c) and (1d), we can get two sets of the $\triangle a_1$, $\triangle a_2$, $\triangle b_1$, and $\triangle b_2$, noted as $\triangle a^{n(n=1,2)}_{m(m=1,2)}$, and $\triangle b^{n(n=1,2)}_{m(m=1,2)}$ for convenience. Now we give the criterion to find the roots of the equation. If the a and b are the roots of the complex equation satisfying $f(a,b) = 0$, then

$$\begin{cases} \triangle a^{n(n=1,2)}_{m(m=1,2)} > 0, & \triangle b^n_m > 0, \\ \triangle a^1_{m(m=1,2)} = \triangle a^2_{m(m=1,2)}, & \triangle b^1_{m(m=1,2)} = \triangle b^2_{m(m=1,2)}, \end{cases} \quad (4a)$$

must be held. Or, there exists no root in the grid A due to the $f(a,b) \neq 0$ in eq.(1). Considering the error allowance δ, criterion (4a) can be modified as

$$\begin{cases} \triangle a^{n(n=1,2)}_{m(m=1,2)} > 0, & \triangle b^n_m > 0, \\ \left|\frac{\triangle a^1_{m(m=1,2)} - \triangle a^2_{m(m=1,2)}}{\triangle a^2_{m(m=1,2)}}\right| < \delta, & \left|\frac{\triangle b^1_{m(m=1,2)} - \triangle b^2_{m(m=1,2)}}{\triangle b^2_{m(m=1,2)}}\right| < \delta. \end{cases} \quad (4b)$$

By using this method, the correct mesh enclosing the root can be found. And then we can further gird the correct mesh and consider the grid point with the minimum value of $|f(x,y)|$ in

the mesh as the root of the equation, at least they are very close to the roots. We note that in our method the criterion $|f(x_0, y_0)| < \delta$ is not fatal for the determination of the roots. And the function values $|f(x, y)|$ at the points considered as the roots may be larger than the error allowance δ if one wants to save computation time. The criterion (4) can guarantee the points close to the exact roots if the points are enclosed in the correct meshes satisfying the criterion (4). In our method, all the meshes are independent to each other. Thus, all possible roots can be found, overcoming the problem met by the NR method. What is more, this method focuses on the finding of correct meshes enclosing the roots instead of the finding of correct points matching the roots, which saves much more computation time.

B. parabola approximation

Generally, if the derivative $f'_{x(y)}(x, y)$ in eq.(1) may equal to zero when the function $f(x, y)$ has a parabola-like shape, we can expand the function with the Taylor series up to order two

$$\begin{aligned} f(x,y) = \quad & f(c,d) + f_{1x}(c,d)\triangle c + f_{1y}(c,d)\triangle d \\ & + f_{2xx}(c,d)\triangle c^2 + f_{2yy}(c,d)\triangle d^2 + f_{2xy}(c,d)\triangle c\triangle d. \end{aligned} \tag{5}$$

Here, $f_{1x(y)}$ is the coefficient for the first order Taylor expansion and the $f_{2x(y)x(y)}$ is the coefficient for the second order. If the c and d are the roots of the complex equation, then $f(c, d) = 0$ is held. For illustration, point (c, d) is enclosed in the mesh B, shown in the fig. 1. Each point of mesh B used for the calculation has been labeled by $j(j = 1, 2, 3, 4, 5, 6, 7, 8)$ in the fig.1. Then, we can get

$$f_{2xy}(c,d) = \frac{f(x,y)_2 + f(x,y)_3 - f(x,y)_1 - f(x,y)_4}{S_x S_y}, \tag{6a}$$

and two sets of the $f_{2xx}(c, d)$ and $f_{2yy}(c, d)$, noted as $f_{2xx}^{n(n=1,2)}(c, d)$ and $f_{2yy}^{n(n=1,2)}(c, d)$:

$$\begin{cases} f^1_{2xx}(c,d) = \frac{2(f(x,y)_1 + f(x,y)_2) - 4f(x,y)_5}{S_x^2}, \\ f^1_{2yy}(c,d) = \frac{2(f(x,y)_3 + f(x,y)_1) - 4f(x,y)_6}{S_y^2}, \end{cases} \tag{6b}$$

and

$$\begin{cases} f^2_{2xx}(c,d) = \frac{2(f(x,y)_3 + f(x,y)_4) - 4f(x,y)_8}{S_x^2}, \\ f^2_{2yy}(c,d) = \frac{2(f(x,y)_2 + f(x,y)_4) - 4f(x,y)_7}{S_y^2}. \end{cases} \tag{6c}$$

Here, the subscript j of $f(x, y)_j$ specifies the function $f(x, y)$ calculated at the point j of the mesh B. After some algebra, we get the following linear equation system:

$$\begin{aligned} & f_{1x}(c,d) - 2f_{2xx}(c,d)\triangle c_1 + f_{2xy}(c,d)\triangle d_1 \\ & \quad = \frac{4f(x,y)_5 - 3f(x,y)_1 - f(x,y)_2}{S_x}, \end{aligned} \tag{7a}$$

$$\begin{aligned} & - f_{1y}(c,d) - 2f_{2yy}(c,d)\triangle d_1 + f_{2xy}(c,d)\triangle c_1 \\ & \quad = \frac{4f(x,y)_6 - 3f(x,y)_1 - f(x,y)_3}{S_y}. \end{aligned} \tag{7b}$$

The eq.(7a) and (7b) are complex. Each equation can be separated into two equations with respect to the real and imaginary parts of the equation. Now we consider three situations. The first situation is $f_{1x}(c, d) = 0$. The second situation is $f_{1y}(c, d) = 0$. And the third is both $f_{1x}(c, d) = 0$ and $f_{1y}(c, d) = 0$. For the first situation, we can substitute eq.(6) into the eq.(7a) and get two sets of $\triangle c_1$ and $\triangle d_1$, noted as $\triangle c_1^{p(p=1,2)}$ and $\triangle d_1^{p(p=1,2)}$. And for the second situation, by substituting eq.(6) into eq.(7b), we also obtain two sets of $\triangle c_1$ and $\triangle d_1$, noted as $\triangle c_1^{p(p=3,4)}$ and $\triangle d_1^{p(p=3,4)}$. Last, for the third situation, we then can get four sets of the roots $\triangle c_1^{p(p=1,2,3,4)}$ and $\triangle d_1^{p(p=1,2,3,4)}$ from the eq.(7). Now we give the criterion to find roots of the equation. If the c and d are the roots of the complex equation satisfying $f(c, d) = 0$, then for the eq.(6) the criterion

$$\begin{cases} \left| \frac{f^1_{2xx} - f^2_{2xx}}{f^1_{2xx}} \right| < \delta, \\ \left| \frac{f^1_{2yy} - f^2_{2yy}}{f^1_{2yy}} \right| < \delta, \end{cases} \tag{8a}$$

must be held. And for the first situation of $f_{1x}(c, d) = 0$, additional criterion is

$$\begin{cases} \left| \frac{\triangle c_1^1 - \triangle c_1^2}{\triangle c_1^1} \right| < \delta, \\ \left| \frac{\triangle d_1^1 - \triangle d_1^2}{\triangle d_1^1} \right| < \delta. \end{cases} \tag{8b}$$

For the second situation of $f_{1y}(c, d) = 0$, the additional criterion is

$$\begin{cases} \left| \frac{\triangle c_1^3 - \triangle c_1^4}{\triangle c_1^3} \right| < \delta, \\ \left| \frac{\triangle d_1^3 - \triangle d_1^4}{\triangle d_1^3} \right| < \delta. \end{cases} \tag{8c}$$

And for the third situation of both $f_{1x}(c, d) = 0$ and $f_{1y}(c, d) = 0$, the additional criterions of eq.(8b) and (8c) both should be held.

III. CALCULATION AND DISCUSSION

A. dispersion equation

In order to verify our method, the complex dispersion equation of SPPs on the planar metallic surface has been investigated. The rigorous analytical solutions to the dispersion equation[11–14] in that case have confirmed the validity of our method. However, in this paper we focus our attention on the solutions to the dispersion equation of a cylindrical metallic nanowire. The nanowire has the shape with the radius of r and an infinite length in a medium. The electromagnetic field

can be expanded with cylindrical harmonics. By solving the Maxwell equation with the boundary conditions imposed, the dispersion equation can be obtained as the following transcendental equation:

$$\begin{vmatrix} H_n^{(1)}(k_{r0}r)k_{r0}^2 & 0 & -J_n(k_{r1}r)k_{r1}^2 & 0 \\ 0 & H_n^{(1)}(k_{r0}r)k_1k_{r0}^2 & 0 & -J_n(k_{r1}r)k_0k_{r1}^2 \\ k_{r0}rH_n^{(1)\prime}(k_{r0}r)k_0k_1 & -nk_zH_n^{(1)}(k_{r0}r)k_1 & -k_{r1}rJ_n'(k_{r1}r)k_0k_1 & nk_zJ_n(k_{r1}r)k_0 \\ -nk_zH_n^{(1)}(k_{r0}r) & k_{r0}rH_n^{(1)\prime}(k_{r0}r)k_0 & nk_zJ_n(k_{r1}r) & -k_{r1}rJ_n'(k_{r1}r)k_1 \end{vmatrix} = 0, \tag{9}$$

which repeats the reported results.[15,17] Here, $H_n^{(1)}$ is the first kind of Hankel function with the order of integer n and J_n is the Bessel function of nth order. The Hankel and Bessel functions with denote represent the first order differentiation. $k_{j(j=0,1)}$ is the wave vector with the value of $k_j = \sqrt{\varepsilon_j}\omega/c$, where $\varepsilon_j$is the dielectric function and the subscript j labels the quantities outside the nanowire ($j = 0$) or inside it ($j = 1$). c is the speed of light in vacuum. The dielectric function of the metal can be expressed as

$$\varepsilon_1(\omega) = \varepsilon_\infty[1 - \frac{\omega_p^2}{\omega(\omega + i\tau)}], \tag{10}$$

where ω_p is the bulk-plasmon frequency and τ is the bulk electron relaxation rate,[18] which reflects the metal Ohmic loss. Eq.(9) then is a complex equation with τ introduced into the dielectric. ε_∞ in eq.(10) is a constant for the general description of the dielectric function of the metal. k_z is the component of the SPPs wave vector along the cylinder axial and the radial components of the wave vectors are defined as $k_{rj} = \sqrt{k_j^2 - k_z^2}$. We note that the value of k_{r0} should be chosen to guarantee the imaginary part of k_{r0} to be positive since the light intensity should be decaying away from the metal cylinder. The dispersion relation between k_z and ω then can be obtained from the eq.(9) numerically. For the calculation, we renormalize the ω and τ by ω_p. Wave vector components of $k_{j(j=0,1)}$, k_z and $k_{rj(j=0,1)}$ are renormalized by ω_p/c and r is renormalized by c/ω_p.

B. $complex - \omega$ solution

Fig. 2 shows the $complex-\omega$ dispersion relations calculated from the eq.(9) by using our method. For the comparison between the published results[18] and our results, the dielectrics take the values of $\epsilon_0 = 5.3$ and $\epsilon_\infty = 9.6$ with $\tau = 0.005647$ in the calculation. The renormalized radius r takes the value of $r = 0.5$ for the nanowire, which is corresponding to the real radius of $26.9nm$. Four orders ($n = 0, 1, 2, 3$) of the dispersion relations are calculated. The left column of the figures is for the relation of $Re[\omega]$ and k_z and the right column is for the relation of $Im[\omega]$ and k_z. In the calculation, the mesh size is 0.01 and the error allowance δ is set to be $\delta = 0.1$. It is shown that there exist two dispersion branches in the figures of $n = 0$ and $n = 1$, shown in figs. 2(a)-(d). One branch is an asymptotic curve with the frequency approaching the surface plasmon frequency $\omega_{sp} = \sqrt{\epsilon_\infty/(\epsilon_0 + \epsilon_\infty)} \approx 0.8$, which represents the SPPs surface wave. Another branch having the frequency above 1 is not a surface wave but identified as the locus of the Brewster angle.[12] In our calculation, the SPPs dispersion curve are found by the using of the criterion (4) while the locus of the Brewster angle needs the criterion (8), reflecting that the relation between the k_z and $Re[\omega]$ behaves parabola-like when it is close to the locus of the Brewster angle. For the order $n > 1$, the relation between the ω and k_z is nearly dispersionless and no locus of the Brewster angle can be observed anymore. The imaginary parts of the frequencies are very small, which have been shown in the right figures. Our calculated results are coincident to the published results,[18] confirming the validity of our method. Our results exhibit that two dispersion branches can be obtained in once calculation by our method, however, which can not be achieved by the NP method if the frequency range includes the two curves.

C. $complex - k$ solution

We have repeated the reported results[19] by using our method with $\epsilon_0 = 1$, $\epsilon_\infty = 1$, $\tau = 0.039062$ and $n = 1$. However, we only show our result with $n = 0$ in fig. 3 since in this case an approximate analytical solution can be derived to verify our calculated results. The renormalized radius of the nanowire for the calculation is $r = 2$, which is corresponding to the real radius of $105nm$.[19] By using our method, full solutions to the complex dispersion equation can be obtained, exhibiting many modes in fig. 3(a) and (b). Those modes can be classified into three, which have been shown in fig. 3(c)-(h). Each figure in the left side responses for the relation of ω and $Re[k_z]$, and the corresponding figure at its right side is for the relation of ω and $Im[k_z]$. Dispersion curves in fig. 3(c) and (d) exhibit the locus of the Brewster angle.[12] Fig. 3(e) and (f) represent the SPPs mode with a back bending in the curve. The back bending is induced by the metal loss.[24] For a nanowire fabricated with perfect metal, the SPPs mode then is an asymptotic curve to infinity when the frequency approaches the $\omega_{sp} = 1/\sqrt{2}$. The third class of the modes in fig. 3(g) and (h) have an infinite mode number and the $Re[k_z]$ of those modes are small compared to $Im[k_z]$. Those modes have been defined as bulk modes (BMDs),[19] but never been reported in this case. Therefore, there exists one question that if the BMDs are wrong solutions in our calculation. To answer this question, we derive an approximate solution to the complex dispersion equation in the following to verify our method.

Before the derivation, three main characteristics of the calculated BMDs should be clarified. The first characteristic is that the dispersion curves of the BMDs are all nearly parallel to the ω axis, meaning that $Im[k_z]$ of the BMDs are independent to ω. The second is that the dispersion curves of the BMDs have a period of $\triangle\, Im[k_z]\times r \approx \pi$. Here, $\triangle\, Im[k_z]$ is the interval between the curves. The third characteristic is that the lower dispersion curves with $\omega < \omega_{sp}$ shift their phases by $\triangle\, Im[k_z] \times r \approx \pi/2$ with respect to the upper curves of $\omega > \omega_{sp}$.

For the derivation, it is reasonable for us to consider the limit case of $Re[k_z] \to 0$ and $Im[k_z] \to \infty$ based on fig. 3(g) and (h). Thus, the Bessel and Hankel functions in eq.(9) can

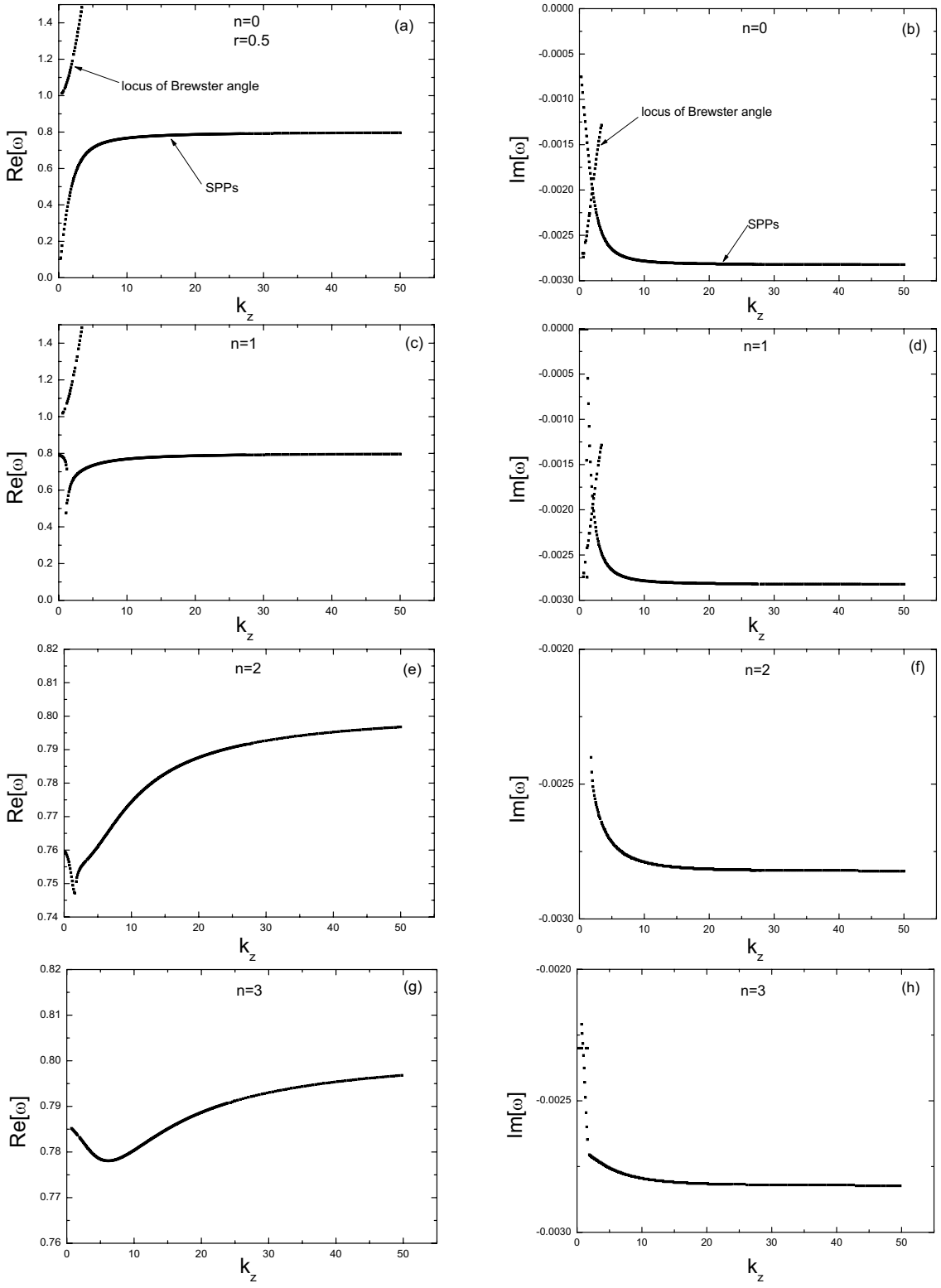

FIG. 2: *complex*$-\omega$ dispersion relations calculated by our method for a cylindrical metallic nanowire with $\epsilon_0 = 5.3$, $\epsilon_\infty = 9.6$ and $\tau = 0.005647$. The renormalized radius $r = 0.5$ is used for the calculation, which is corresponding to the real radius of 26.9*nm* of the nanowire.

be replaced by

$$J_0(t) \approx \sqrt{\frac{2}{\pi t}} cos(t - \frac{\pi}{4}), \tag{11a}$$

$$H_0^{(1)}(t) \approx \sqrt{\frac{2}{\pi t}} e^{i(t-\pi/4)}. \tag{11b}$$

And to get the analytical solution, $k_{r\,j(j=0,1)}$ should be ex-

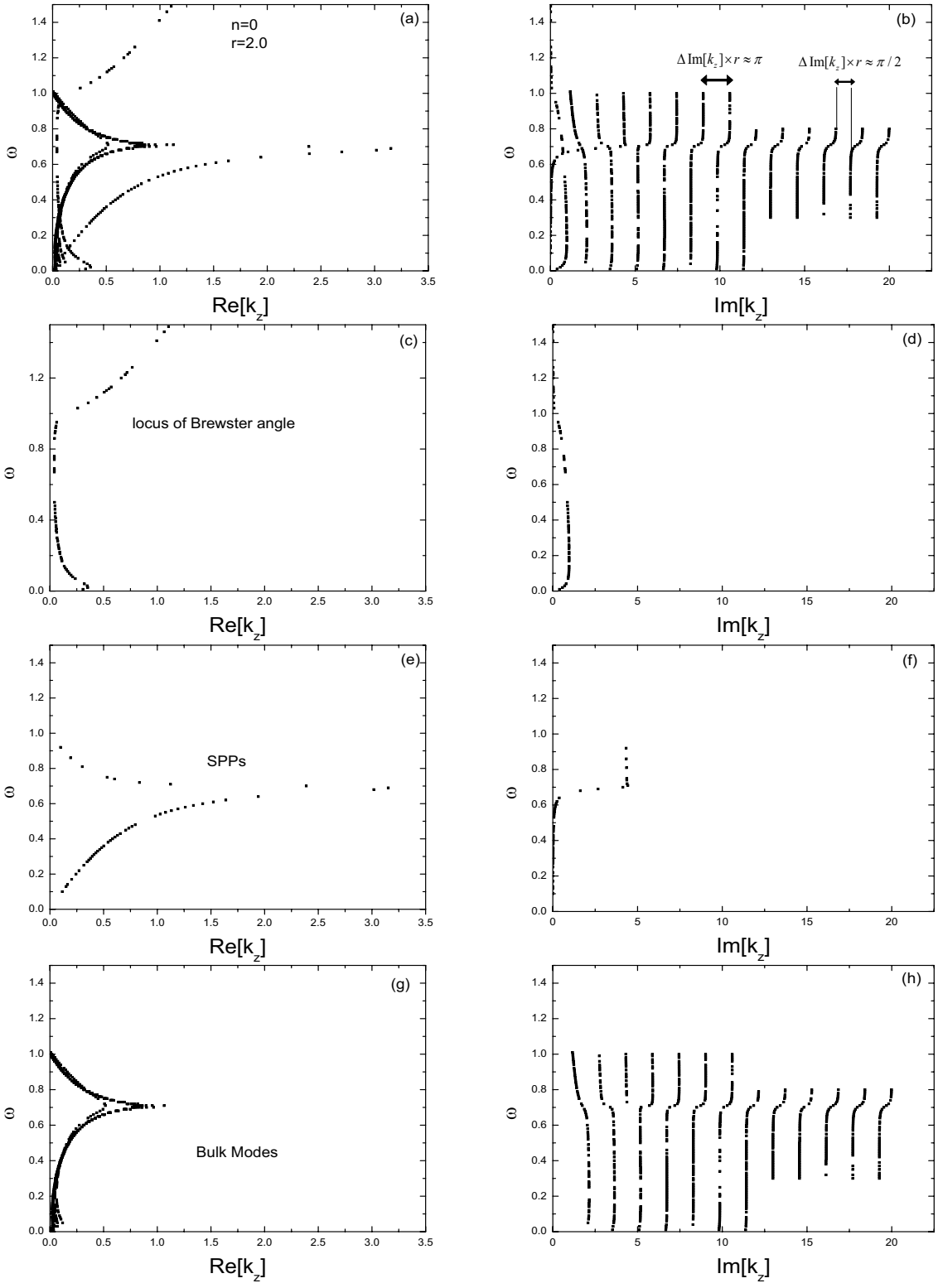

FIG. 3: *complex* − *k* dispersion relations calculated by our method for a cylindrical metallic nanowire with $\epsilon_0 = 1$, $\epsilon_\infty = 1$ and $\tau = 0.039062$. In the calculation, $r = 2$ and $n = 0$ are used. The renormalized radius $r = 2$ is corresponding to the real radius of 105*nm* of the nanowire.

panded by k_z as

$$k_{rj} \approx \frac{2k_z^2 - k_j^2}{2ik_z}. \qquad (11c)$$

For simplicity, the metal is assumed to be perfect with $\tau = 0$. Substituting eqs.(11)into eq.(9), we can get a simple equation

$$e^{-Re[k_z]\times r - i(Im[k_z]\times r - \frac{\pi}{4})} \approx (\pm)\gamma, \qquad (12)$$

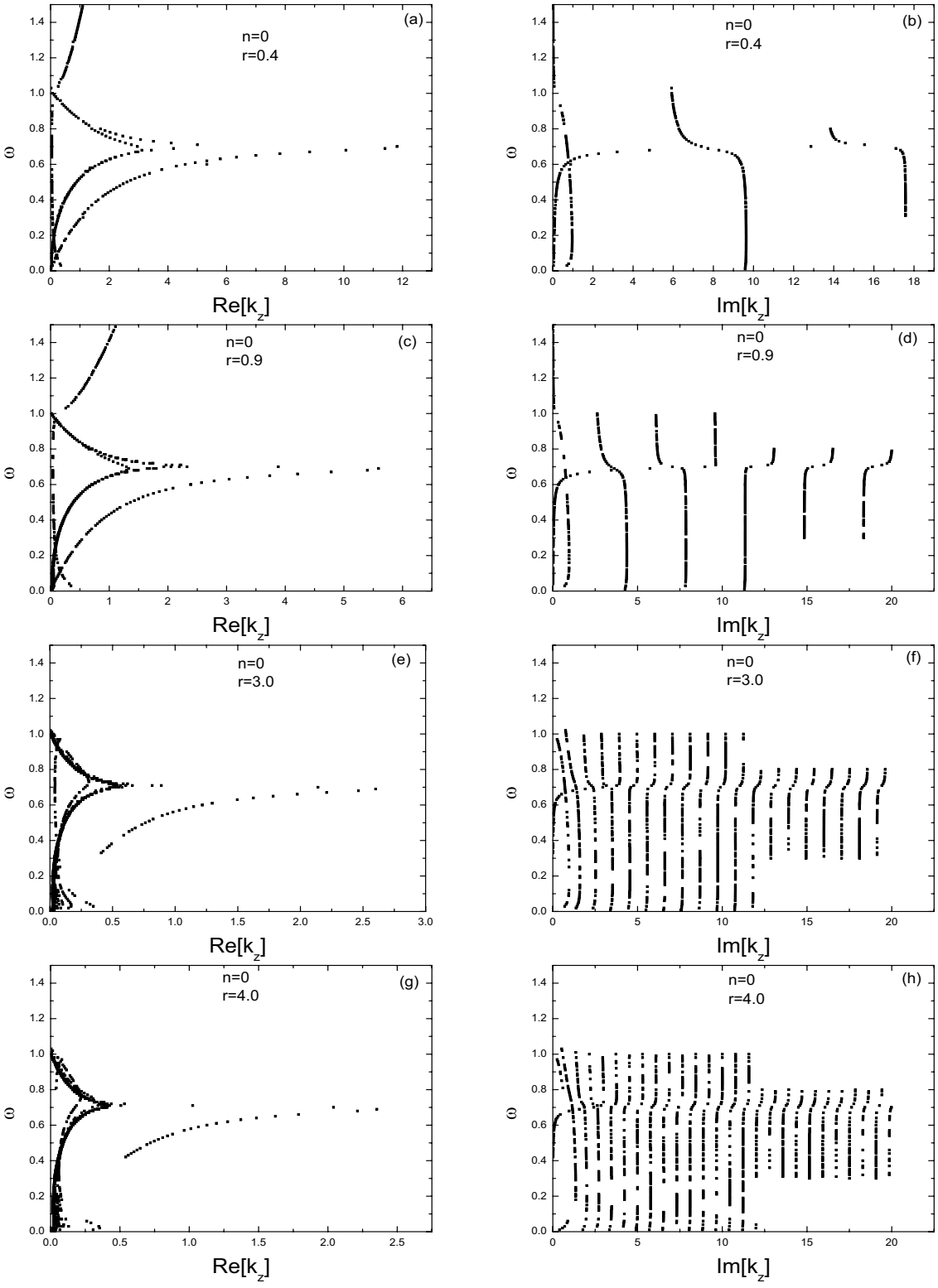

FIG. 4: *complex – k* dispersion relations calculated by our method for cylindrical metallic nanowires with various radius *r*. In the calculation, $\epsilon_0 = 1$, $\epsilon_\infty = 1$, $n = 0$ and $\tau = 0.039062$ are used.

with

$$\gamma = \frac{1 - \omega^2 \pm \omega}{\sqrt{1 - 2\omega^2}}.$$

For the lower dispersion curves, considering $+\gamma$ at the right

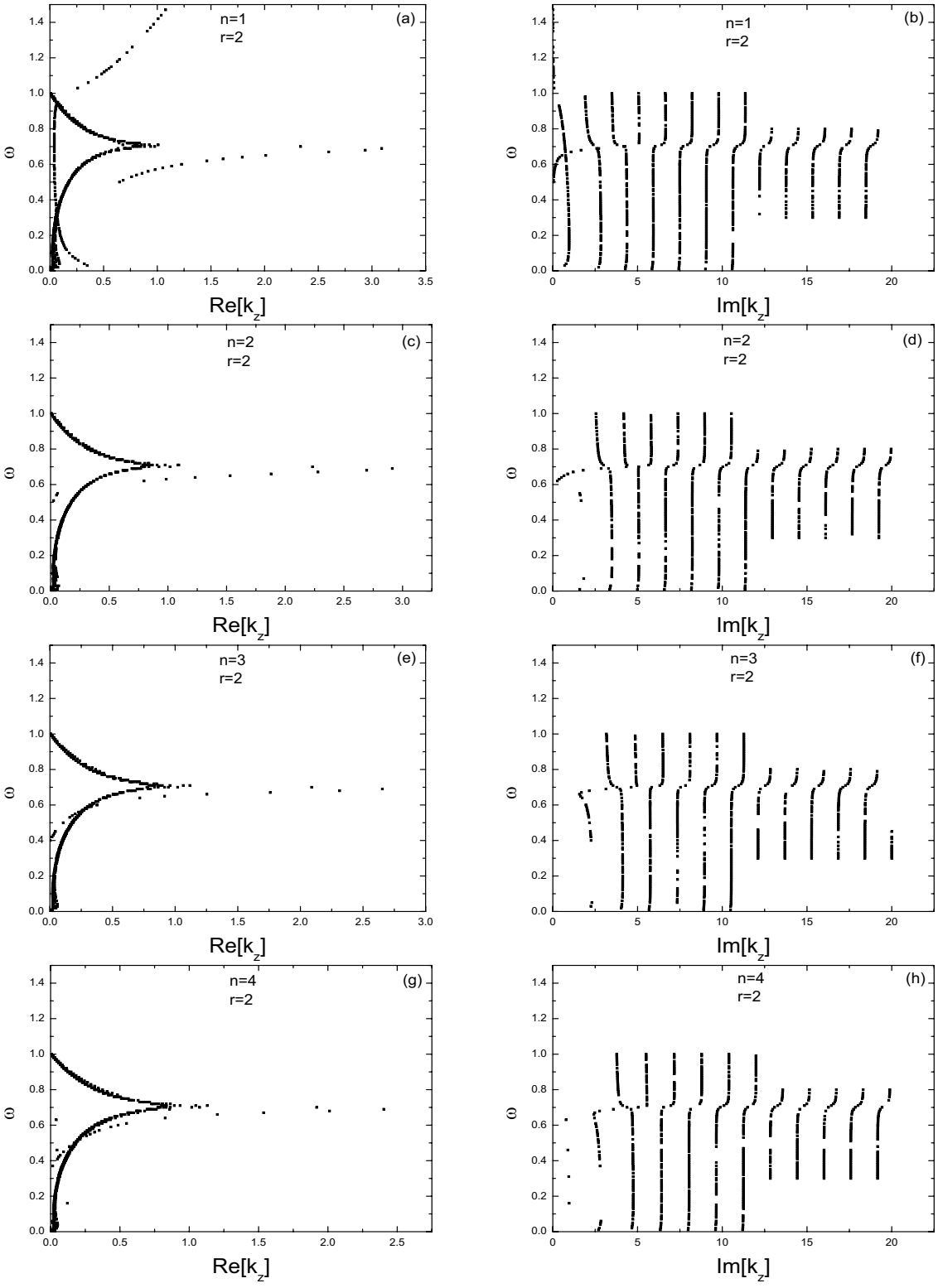

FIG. 5: *complex – k* dispersion relations calculated by our method for a cylindrical metallic nanowire with various orders *n*. In the calculation, $\epsilon_0 = 1$, $\epsilon_\infty = 1$, $r = 2$ and $\tau = 0.039062$ are used.

side of eq.(12), the complex k_z can be solved analytically as

$$\begin{cases} Re[k_z] = -\frac{\ln(|\gamma|)}{r}, \\ Im[k_z] = \frac{\pi/4+2m\pi}{r}. \end{cases} \tag{13}$$

In eq.(13), m is an integer. Due to the approximation in the derivation, the analytical solutions are not coincident to the calculated results of the BMDs. However, we find that in the

analytical solutions the $Im[k_z]$ is independent to the ω, which is the first characteristic of the BMDs we calculated. Secondly, the analytical solution of $Im[k_z]$ shows that the solutions have a period of $\triangle\ Im[k_z] \times r = 2\pi$. Considering the minus before γ in the right side of eq.(12), the period is then equal to $\triangle\ Im[k_z] \times r = \pi$, which is the second characteristic of the calculated BMDs results. Last, for the upper curves with $\omega > 1/\sqrt{2}$, the denominator of γ is a pure imaginary value, which is equivalent to the phase shift of $\triangle\ Im[k_z] \times r$ by $\pi/2$ with respect to the lower curves. This conclusion is just the third characteristic of the BMDs results calculated by our method. Thus, the approximate analytical solution to the eq.(9) confirms the validity of our method. As shown in fig.3, full solutions to the complex dispersion equation can be obtained in once calculation by our proposed method.

In the derivation, $\tau = 0$ means that the BMDs are induced by the structure formation instead of metal loss. For details, fig. 4 shows the dispersion curves of BMDs with various r in the case of $n = 0$, $\epsilon_0 = 1$, $\epsilon_\infty = 1$, and $\tau = 0.039062$. The curves have two peaks with peak one close to the surface plamson frequency and peak two at low frequency. For the nanowires with a smaller radius r, the $\triangle\ Im[k_z]$ is larger to hold the period $\triangle\ Im[k_z] \times r = \pi$. In this case, peak one is larger while peak two smaller. We also find that the period is the basic property of the BMDs, which is independent to the integer order n. The BMDs for different orders has been presented in fig. 5, showing the $Im[k_z]$ of BMDs have the same period but different position.We suggest that the order n only influences the initial position of $Im[k_z]$.

IV. SUMMARY

We have proposed one new method to find full complex roots of a complex transcendental equation. The correct meshes enclosing the roots are independent to each other, which guarantee the finding of the all roots. For the application of this method, the complex dispersion equation of a cylindrical metallic nanowire is investigated. In our calculation, locus of the Brewster angle, SPPs dispersion curves, and bulk modes all can be obtained in once calculation. Approximate analytical solution to the dispersion equation has been derived to verify our results. This method can be applied to all other complex transcendental equations with two real variables.

* Electronic address: liwan˙china@yahoo.com.cn

[1] W. L. Barnes, A. Dereux, and T. W. Ebbesen, Nature(London) **424**, 824 (2003).
[2] S. Maier and H. Atwater, J. Appl. Phys **98**, 011101 (2005).
[3] E. Ozbay, Science **311**, 189 (2006).
[4] S. Lal, S. Link, and N. J. Halas, Nature Photon. **1**, 641 (2007).
[5] D. K. Gramotnev and S. I. Bozhevolnyi, Nature Photon. **4**, 83 (2010).
[6] C. E. Talley, J. B. Jackson, C. Oubre, N. K. Grady, C. W. Hollars, S. M. Lane, T. R. Huser, P. Nordlander, and N. J. Halas, Nano Lett. **5**, 1569 (2005).
[7] E. Prodan, C. Radloff, N. J. Halas, and P. Nordlander, Science **302**, 419 (2003).
[8] K. L. Kelly, E. Coronado, L. L. Zhao,a nd G. C. Schatz, J. Phys. Chem. B **107**, 668 (2003).
[9] F. J. Garcia de Abajo and M. Kociak, Phys. Rev. Lett. **100**, 106804 (2008).
[10] C. Chicanne, T. David, R. Quidant, J. C. Weeber, Y. Lacroute, E. Bourillot, A. Dereux, G. Colas des Francs, and C. Girard, Phys. Rev. Lett. **88**, 097402 (2002).
[11] R. Ruppin, *Electromagnetic Surface Modes* (Wiley, Chichester, 1982).
[12] A. Archambault, T. V. Teperik, F. Marquier, and J. J. Greffer, Phys. Rev. B **79**, 195414 (2009).
[13] P. Halevi, *Electromagnetic Surface Modes* (Wiley, Chichester, 1982).
[14] S. A. Rice, D. Guidotti, and H. L. Lemberg, *Aspects of the Study of Surfaces* (Wiley, New York, 1974).
[15] C. A. Pfeiffer, E. N. Economou, and K. L. Ngai, Phys. Rev. B **10**, 3038 (1974).
[16] J. C. Ashley and L. C. Emerson, Surf. Science bf 41, 615 (1974).
[17] D. E. Chang, A. S. Sϕrensen, P. R. Hemmer, M. D. Lukin, Phys. Rev. Lett. **97**, 053002 (2006); D. E. Chang, A. S. Sϕrensen, P. R. Hemmer, M. D. Lukin, Phys. Rev. B **76**, 035420 (2007).
[18] Y. N. Chen, G. Y. Chen, D. S. Chuu, and T. Brandes, Phys. Rev. A **79**, 033815 (2009).
[19] L. Novotnv and C. Hafner, Phys. Rev. E **50**, 4094 (1994).
[20] E. T. Arakawa, M. W. Williams, R. N. Hamm, and R. H. Ritchie, Phys. Rev. Lett. **31**, 1127 (1973).
[21] R. W. Alexander, G. S. Kovener, and R. J. Bell, Phys. Rev. Lett. **32**, 154 (1974).
[22] Indika B. Udagedara, Ivan D. Rukhlenko, and Malin Premaratne, Phys. Rev. B **83**, 115451 (2011).
[23] Peijun Yao, C. Van Vlack, A. Reza, M. Patterson, M. M. Dignam, and S. Hughes, Phys. Rev. B **80**, 195106 (2009).
[24] Li Wan, Yun-Mi Huang, Chang-Kun Dong, Hai-Jun Luo, arXiv:1108.4797v1.